

An Optimized Encoding Scheme for Planning Vessel-Encoded Pseudocontinuous Arterial Spin Labeling

Eleanor S. K. Berry, Peter Jezzard, and Thomas W. Okell*

Purpose: Vessel-encoded pseudocontinuous arterial spin labeling allows the acquisition of vessel-selective angiograms and vascular territory perfusion maps. The technique generates a periodic variation in inversion efficiency across space that can be manipulated to encode specific combinations of vessels. Currently, the choice of these encodings is limited to scenarios with few vessels and may not optimize the signal-to-noise ratio (SNR). Here we present an automated, rapid method for calculating a minimal number of SNR optimal encodings for any number and arrangement of vessels.

Theory and Methods: The proposed optimized encoding scheme (OES) is a Fourier-based method that finds SNR optimized encodings to best match the ideal encodings for a set of vessels. For nine or fewer vessels, the calculation takes less than 3 s.

Results: In simulations, the OES method produces encodings for a range of vessel geometries that, on average, have an SNR efficiency 37% greater than that for random encoding. When labeling vessels in the neck in healthy subjects, the OES encodings result in images with higher SNR than other encoding methods.

Conclusion: The OES results in a minimal number of encodings with a higher SNR efficiency than other encoding methods, regardless of the number or geometry of the vessels.

Magn Reson Med 74:1248–1256, 2015. © 2014 The Authors. Magnetic Resonance in Medicine Published by Wiley Periodicals, Inc. on behalf of International Society of Medicine in Resonance. This is an open access article under the terms of the Creative Commons Attribution License, which permits use, distribution, and reproduction in any medium, provided the original work is properly cited.

Key words: vessel-encoded pseudocontinuous arterial spin labeling; vessel-selective; encoding scheme; SNR efficiency; perfusion

INTRODUCTION

Vessel-selective angiograms and vascular territory maps allow collateral circulation in the brain to be visualized. Knowledge of collateral circulation can help the understanding and potential treatment of stroke and other cerebrovascular diseases (1,2). Vessel selectivity also allows the assessment of blood supply to lesions such as arteriovenous malformations and tumors.

The gold standard for acquiring vessel-selective information is X-ray digital subtraction angiography. X-ray digital subtraction angiography is an invasive method, requiring both the insertion of a catheter to administer a contrast agent, carrying an associated risk of stroke or transient ischemic attack (3), and the use of ionizing radiation (4).

Vessel-selective arterial spin labeling is a noninvasive method for acquiring angiograms (5) and perfusion information in the brain. Vessel selectivity can be achieved in a variety of ways. For example, single vessels can be selected, or tagged, using localized radiofrequency pulses or via modulation of gradient waveforms (6–9). Alternatively, slabs containing only the artery or arteries of interest can be inverted (10–13). However, single artery selective methods are not signal-to-noise ratio (SNR) efficient when multiple arteries are of interest.

With vessel-encoded pseudocontinuous arterial spin labeling (VEPCASL) the labeling efficiency varies periodically across the plane in which vessels are tagged. The spatial frequency and phase of this “encoding function” can be adjusted to allow different combinations of vessels to be tagged and controlled for any given measurement (14). Pseudocontinuous arterial spin labeling has been shown to have higher SNR than pulsed arterial spin labeling (15), and VEPCASL yields an SNR comparable to that of standard pseudocontinuous arterial spin labeling (16). Additionally, compared with other vessel-selective methods, VEPCASL is capable of labeling vessels that are closer together (17).

VEPCASL can be performed without prior knowledge of the vessel locations by random encoding—that is, applying many random encoding functions to the labeling plane and combining the images to get vessel specific information (18). The random technique removes the need for user selection of vessels but requires the acquisition of more encoding cycles than would otherwise be necessary and thus reduces the achievable SNR efficiency. Planning-free VEPCASL is also possible, where a few fixed encodings are applied and vascular territory information is achieved using a voxel clustering method (19). The SNR efficiency of this method is vulnerable to the geometry of the vessels being labeled and is only designed to label four vessels in the neck.

Alternatively, it is possible to empirically choose a set of encoding functions that work relatively well in

Centre for Functional Magnetic Resonance Imaging of the Brain, Nuffield Department of Clinical Neurosciences, University of Oxford, Oxford, UK.

Grant sponsor: Engineering and Physical Sciences Research Council and The Dunhill Medical Trust.

*Correspondence to: Dr. Thomas Okell, FMRI Centre, John Radcliffe Hospital, Headington, Oxford, OX3 9DU, UK. E-mail: thomas.okell@ndcn.ox.ac.uk

The copyright line for this article was changed on 9 December 2014 after original online publication.

Received 24 July 2014; revised 26 September 2014; accepted 3 October 2014

DOI 10.1002/mrm.25508

Published online 28 October 2014 in Wiley Online Library (wileyonlinelibrary.com).

© 2014 The Authors. Magnetic Resonance in Medicine Published by Wiley Periodicals, Inc. on behalf of International Society of Medicine in Resonance. This is an open access article under the terms of the Creative Commons Attribution License, which permits use, distribution, and reproduction in any medium, provided the original work is properly cited.

© 2014 Wiley Periodicals, Inc.

specific scenarios (16). For example, in the case of four vessels, an ideal encoding can be achieved if the vessels are approximately in a rectangular formation. However, such a perfectly encoded situation is rarely encountered in practice. If there are more than four vessels, achieving ideal encodings becomes increasingly difficult. Computational methods that attempt to find the most SNR-efficient encodings are also possible (20) but require extra calculation time that may not be possible in a clinical setting. As such, there is currently no method for automatically and rapidly calculating a minimal number of SNR-efficient encodings for nonregular arrangements of more than three vessels. We propose a rapid optimized encoding scheme (OES) that automates the choice of SNR-efficient encodings, regardless of the number or arrangement of vessels. This builds on work previously presented in abstract form (21).

THEORY

Encoding Schemes

An encoding scheme specifies which arteries are tagged or controlled during a given VEPCASL encoding cycle. The encoding matrix is the mathematical description of the encoding scheme from which the SNR efficiency can be derived according to Wong (14). The signal within each voxel is described mathematically as:

$$\mathbf{y} = \mathbf{A} \cdot \mathbf{x} \quad [1]$$

where \mathbf{y} is the vector of measured signal intensities for all encoding cycles, \mathbf{A} is the encoding matrix, and \mathbf{x} is the unknown vector describing the signal contributions from each vessel plus static tissue (14).

Ideal encoding matrices are those whose SNR efficiency is equal to one for all vessels (14), which requires that the arteries are perfectly tagged (-1) and controlled ($+1$) an equal number of times. An example ideal encoding matrix for four vessels in the neck, described by Okell et al. (16), is shown below. The columns describe (from left to right) the label/control state of the right internal carotid artery, left internal carotid artery, right vertebral artery, left vertebral artery, and static tissue, respectively, for each encoding (or row).

$$\mathbf{A} = \begin{bmatrix} -1 & -1 & -1 & -1 & 1 \\ 1 & 1 & 1 & 1 & 1 \\ -1 & 1 & -1 & 1 & 1 \\ 1 & -1 & 1 & -1 & 1 \\ -1 & -1 & 1 & 1 & 1 \\ 1 & 1 & -1 & -1 & 1 \\ -1 & 1 & 1 & -1 & 1 \\ 1 & -1 & -1 & 1 & 1 \end{bmatrix}$$

The columns of this matrix have come from a Hadamard matrix – an encoding matrix consisting of columns from a Hadamard matrix will always have an SNR efficiency of one (14). The order of a Hadamard

matrix must be 1, 2, or an order of 4. When the number of vessels of interest (plus static tissue) does not match the order of a possible Hadamard matrix, then ideal encodings can be composed of the columns of the Hadamard matrix closest in size to (but greater than) the number of vessels. Consequently, there may be more encodings than are strictly necessary to extract the information about all the vessels. However, these extra encodings give the overall encoding scheme the greatest SNR efficiency.

The OES Method

The OES method automates the choice of the encoding function used to tag/control the arteries of interest in a given VEPCASL cycle. It relies on defining an ideal encoding scheme and finding real encodings that match these as closely as possible. The method is structured as follows:

1. Construct an “image” of the vessel locations. Each vessel is represented by ± 1 , depending on the ideal encoding (Fig. 1a).
2. Zero-pad this “image.”
3. Take its Fourier transform (Fig. 1b).
4. Weight (Eq. 2) and mask the resulting Fourier space to up-weight lower spatial frequencies (Fig. 1c).
5. Find the maximum intensity in this weighted Fourier space (Fig. 1c).

The maximum intensity point in the weighted Fourier space provides the spatial frequency and phase of the optimized encoding function (Fig. 1d). This process is then repeated for each cycle of the ideal encoding scheme.

The algorithm constructs the “image” of the vessels following the manual input of the vessel locations. The vessels, represented by ± 1 , are placed in a matrix of zeros, at positions corresponding to their physical Cartesian coordinates within the labeling plane. Zero-padding the image increases resolution in Fourier space, allowing the optimal spatial frequency to be identified more precisely.

Up-weighting lower spatial frequencies while masking higher ones makes the method more robust to gross subject motion; if a chosen encoding function has a low spatial frequency, then should a subject move, the vessels of interest will remain close to the desired encoding. If the vessels of interest are close together, a larger spatial frequency is required to efficiently differentiate them. However, if the spatial frequency is too high, even a small amount of movement could shift a vessel from a label to a control location, leading to considerable deviation from the desired encoding. In addition, at very high spatial frequencies, there may be considerable variation in inversion efficiency across the diameter of a vessel, thereby reducing the average inversion efficiency and causing further deviations from the expected encoding. The weighting function is present to ensure the algorithm has a tendency to choose lower spatial frequencies where there is a range of possible encoding functions that give a good match to the desired encoding. Note that there is no lower limit on the choice of spatial frequency, since encoding functions with wavelengths

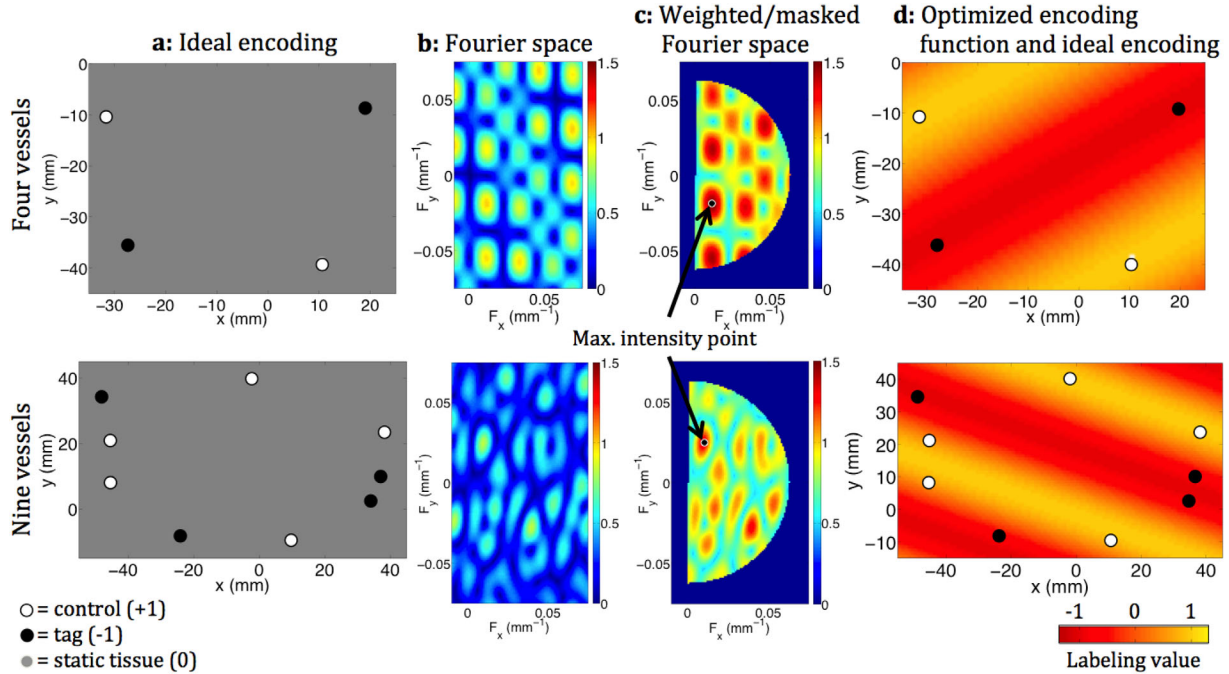


FIG. 1. OES method for four vessels (top row), representative of the main brain-feeding vessels in the neck, and for nine vessels (bottom row), similar to vessels above the circle of Willis. **a:** “Images” of ideally encoded vessels of interest; static tissue is set to zero. **b:** Fourier transforms of the zero-padded “images.” **c:** Weighted and masked Fourier spaces. The maximum intensity points are indicated by arrows. **d:** Optimized encoding functions overlaid onto the ideal encodings.

much larger than the separation of the vessels cannot give a good match to the desired encoding and will therefore be excluded by the algorithm.

In practice, before the maximum intensity point is identified, the absolute value of the Fourier space is taken, normalized to its maximum value, and then the weightings are added. The weighting function is based on the position of each point in the Fourier space. For a given point at a distance f from the center of the Fourier space, the weighting w is:

$$w = \left(\frac{1 - f/f_{\max}}{2} \right) \quad [2]$$

where f_{\max} is the maximum possible distance of any point from the center. The coordinates of the maximum intensity point in the normalized weighted and masked Fourier space give the spatial frequency and direction of the optimum encoding function, with phase extracted from the same point in the unnormalized, unweighted Fourier space.

The radius of the Fourier space mask is set so that the wavelengths of the chosen encoding functions are at least four times the maximum predicted subject motion. This helps to ensure that, should a subject move, a vessel that was intended to be in the tag condition will not be moved in to a control condition and vice versa. The mask radius gives control over the trade-off between SNR efficiency and motion robustness, and can be tailored for each subject group. The mask also removes the redundant symmetric half of Fourier space.

The transverse gradients in the VEPCASL labeling pulse train used in this study are unipolar (18), i.e. for a given

encoding function all have the same amplitude and direction. The inversion efficiency curve that results after subtraction of a label from a control situation is well represented by a sum of three Fourier coefficients (18). The OES method implicitly assumes that the periodic labeling efficiency in VEPCASL is sinusoidal. However, the root mean squared difference between the sum of these coefficients and a perfect sinusoid is small (only 0.12), so errors resulting from this assumption are likely to be minimal. Note that a more precise representation of the encoding function applied during each VEPCASL cycle can be used in postprocessing, allowing the resulting images to be better decoded into vessel-specific maps.

METHODS

The robustness of the OES method was evaluated against two existing encoding methods: “standard” encoding for four vessels in the neck (16) and random encoding (18) through simulations and scans of healthy volunteers.

Encoding Schemes

Standard Method

When labeling the four main brain-feeding arteries in the neck, the encodings were chosen as described by Okell et al. (16):

- left–right (according to the magnet coordinate system) encodings tag/control the internal carotid arteries;

- anterior–posterior tag/control at the average internal carotid/vertebral artery positions;
- diagonal encoding tags the right carotid and left vertebral arteries whilst controlling the other two vessels, and vice versa.

Random Method

The random encodings were taken from those generated by Wong and Guo (18) so a direct comparison could be drawn between the OES method and this existing method. Where random encoding was used, two nonselective tag/control pairs of encodings were acquired along with 58 pairs of random encodings taken from Wong and Guo. A pair refers to the same encoding with a phase shift of 180° .

OES Method

When considering four vessels, the ideal encoding matrix described by Okell et al. (16) was used so that the OES and “standard” methods could be compared directly. When considering more than four vessels, the columns of a Hadamard matrix were used as the ideal vessel-encoding matrix. The calculations of the optimal encodings were performed in MATLAB (MathWorks, Natick, Massachusetts, USA). The calculation time for a set of encodings using a standard laptop was short: <2 s for four vessels and <3 s for nine vessels.

For all OES calculations, the “image” of the vessels was zero-padded into a 1024×1024 matrix to give the most accurate spatial frequencies and phases without unnecessarily increasing the computation time. The expected maximum subject motion was set to 4 mm in all cases, as the predicted motion of healthy volunteers is low. This value results in a Fourier space mask that allows some higher spatial frequencies to be chosen. Consequently, it is possible to differentiate between vessels close together, as would be expected in vessel configurations above the circle of Willis.

Simulations

Simulations were performed in MATLAB to test the robustness of the OES method to variability in the geometry of vessels of interest. Prior to this, the inversion efficiency of the VEPCASL pulse train was simulated from the Bloch equations. Laminar flow and a blood velocity of $0.3 \text{ m}\cdot\text{s}^{-1}$ were assumed and the inversion efficiency was adjusted to take this into account according to Dai et al. (22). Encoding values were then drawn from this curve to give a more accurate representation of the encoding matrices. The SNR efficiency was averaged across all vessels to simplify comparison between the different encoding methods.

Four Vessel Rotation

Four vessels, in an arrangement typical of the main brain-feeding arteries in the neck, were rotated in intervals of 2° up to 90° .

Four Vessel Shifts

Each vessel location in this typical arrangement was perturbed by a random distance and direction. The

perturbations were chosen randomly from normal distributions (mean = 0) with increasing standard deviation.

Above the Circle of Willis Vessel Shifts

Each vessel in a set of nine, representative of the cerebral arteries above the circle of Willis, was perturbed by a random distance and direction. The perturbations were chosen randomly from normal distributions (mean = 0) with increasing standard deviation.

The first two simulations compared the SNR efficiencies of the encodings produced by the OES, standard, and random methods. The final simulation only involved the OES and random methods, as there is no automatic method for calculating encodings for more than four vessels. All simulations were compared with the theoretical SNR efficiency of the random encoding scheme (18).

Subject Scans

Scans were performed on healthy subjects under a technical development protocol that was approved by the local ethics and institutional committees. Data were acquired on a 3T TIM Verio system (Siemens Healthcare, Erlangen, Germany) with a 32-channel head coil. A three-dimensional multislabs time-of-flight angiography sequence was performed at the start of each scan to allow selection of a labeling plane and localization of vessels.

When labeling the four main brain-feeding arteries in the neck, the OES method was compared with the standard and random encoding methods in five healthy subjects (female, $n = 2$; male, $n = 3$; mean age, 26.8 y [range, 23–35 y]). The order of application of the different methods was randomized across subjects. To assess whether the OES method yields improved vascular territory images, regardless of the arrangement of vessels, two scenarios were tested: 1) the subject normally aligned in the scanner and 2) the subject's head rotated to the left or right (10° – 20°).

When considering more than four vessels above the circle of Willis, the OES and random methods were compared for a single subject to assess whether the OES method leads to more accurate identification of vascular territories.

The VEPCASL labeling scheme was combined with a single-shot echo planar readout to acquire perfusion data. The scanning parameters were the same as those used by Okell et al. (16): tag duration = 1.4 s, voxel size = $3.4 \times 3.4 \times 5$ mm, number of measurements = 120, except a single postlabeling delay of 1 s was used. The total number of measurements was kept the same for all types of encodings and all numbers of vessels to ensure a fair comparison. Consequently, the acquisition time for each type of encoding was the same (7.18 min).

In certain cases where visualization of the encodings was desired, the readout region was reduced to a single slice and moved to the labeling plane itself. A single measurement was acquired for each encoding, with a tag duration of 300 ms, postlabeling delay of 16 ms, and repetition time of 500 ms to allow some T_1 recovery. At a “tag” location within the labeling plane, static spins experience repeated radiofrequency pulses with the same phase

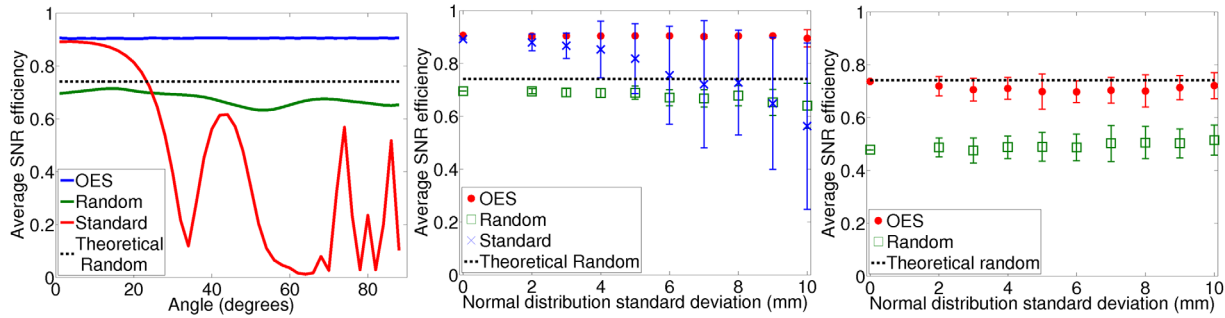


FIG. 2. Simulated average SNR efficiencies in different scenarios. **a:** Four vessels rotated through multiple angles. **b:** Four vessels perturbed by random shifts of increasing magnitude. **c:** Nine vessels perturbed by random shifts of increasing magnitude. Note that there is no “standard” method for encoding this number of vessels.

leading to a saturated and therefore low tissue signal. At a “control” location, static tissue experiences radiofrequency pulses of alternating sign and therefore a relatively high signal. Once a control image is subtracted from an encoded image, the encoding functions are made visible. This allowed the location of the label/control troughs/peaks of the function to be assessed visually.

Image Analysis

Images were averaged across all repeats and analysis was performed in two ways:

Encoding Matrix Inversion

The simplest method of estimating the contribution of different arteries to the signal in a given voxel is to invert (or pseudo-invert) the encoding matrix. The encoding matrix that is achieved during a given measurement deviates from the ideal encoding scheme, so the simulated inversion profile of the blood magnetization following the VEPASL pulse train was used to estimate the actual inversion efficiency at the vessel locations. Once the actual encoding matrix was calculated, it was (pseudo-)inverted to determine the signal arising from each feeding artery.

Bayesian Analysis

A Bayesian, maximum a posteriori (MAP) method was used to separate out vessel-specific information (23). This method considers subsets of the encoding matrix, hence it can deal with poorly conditioned encoding matrices without significant loss of SNR.

Two different comparisons were made: 1) the mean SNR of the vascular territory maps and 2) relative labeling efficiency maps.

Mean SNR of the vascular territory maps. In the vascular territory images obtained through matrix inversion and MAP analysis voxels considered to be within gray matter were used to calculate the SNR across the vascular territories. Only the signal from the dominant feeding vessel in each voxel was used in the calculation. This is consistent with the SNR calculations of Okell et al. (16). The gray matter masks applied to the images were created using partial volume maps for

each subject, obtained with the FMRIB Software Library tool FAST from T₁-weighted structural images (24). These gray matter masks were registered to the VEPASL space using a linear registration (25) and thresholded with a value of 0.5. The SNR was averaged across all subjects and compared for the three encoding methods.

Relative labeling efficiency maps. When four vessels were encoded, the relative labeling efficiency maps were calculated by normalizing the selectively labeled pairs of images to the nonselectively labeled images, identical to the beta parameter described by Wong (14):

$$\beta = \frac{\text{selective tag pair subtraction}}{\text{non selective tag pair subtraction}} \times \text{mask}. \quad [3]$$

The selected tag pair subtraction is, for example, the right-labeled image minus the left-labeled image. The nonselective pair subtraction is the nonselective control minus the nonselective tag image. The mask is a rough gray matter mask calculated by thresholding the nonselective subtraction image. Only voxels with signal above the 99th percentile divided by two were retained. The resulting images show how efficiently the vessels were encoded during each VEPASL cycle.

RESULTS

Simulations

Four-Vessel Rotation

The average SNR efficiency of the OES encodings remained close to the ideal value of one (mean \pm standard deviation [SD] = 0.905 ± 0.001) (Fig. 2a). The average SNR efficiency of the standard encodings shifted away from the ideal after about a 20° rotation (mean \pm SD = 0.429 ± 0.323). The average SNR efficiency of the random encodings was below that of the OES method (mean \pm SD = 0.676 ± 0.025) and close to the theoretical optimal SNR efficiency of random encoding for well-separated vessels (0.74). According to a paired *t* test, the SNR efficiency of the OES encodings was significantly greater than that for the standard ($P \approx 10^{-12}$) and random ($P \approx 10^{-43}$) encodings. Similarly, the random encodings had a significantly greater SNR efficiency than that for standard encoding ($P \approx 10^{-5}$).

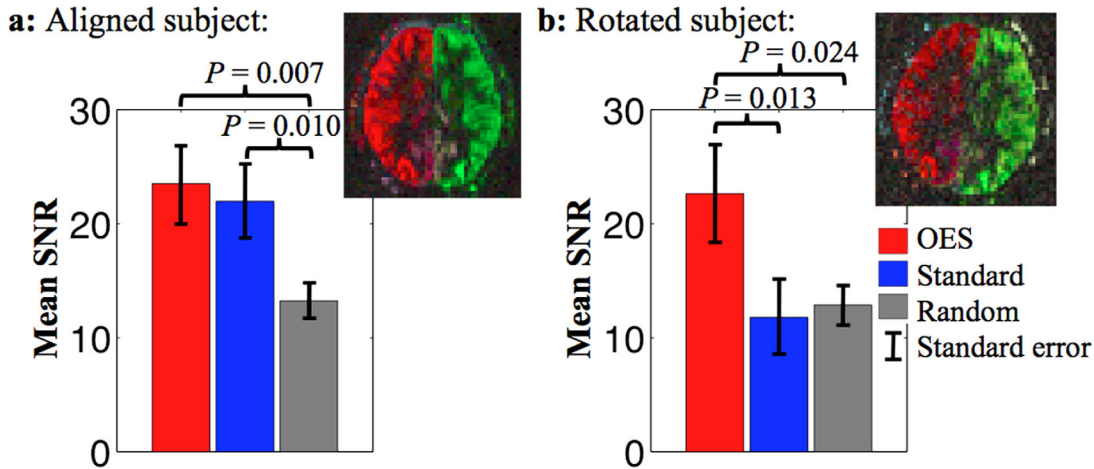


FIG. 3. The mean SNR of the vascular territory images, produced using MI analysis, for five subjects who were aligned with the scanner (a) and rotated (b). The vascular territory images show a single slice following the standard encoding method. The image from the rotated subject is visibly noisier.

Four-Vessel Shifts

As the size of the vessel location perturbation increased, the average SNR efficiency of the OES encodings remained close to the ideal value of one (mean \pm SD = 0.903 ± 0.003), whereas the average SNR efficiency of the standard encodings decreased and became more variable (mean \pm SD = 0.772 ± 0.109) (Fig. 2b). Once again, the average SNR efficiency of the random encodings was below that of the OES method and close to the theoretical value (mean \pm SD = 0.676 ± 0.019). The SNR efficiency of the OES encodings was significantly greater than that for the standard ($P=0.004$) and random ($P \approx 10^{-12}$) encodings, and the SNR efficiency of the standard encodings was significantly greater than that for random encoding ($P=0.009$).

Above the Circle of Willis Vessel Shifts

The average SNR efficiency of the OES encodings was greater than the random encodings in all cases, with a mean \pm SD = 0.710 ± 0.013 for OES encodings and mean \pm SD = 0.492 ± 0.013 for random encodings (Fig. 2c). The SNR efficiency of the two different encoding methods was significantly different ($P \approx 10^{-11}$). The SNR efficiency of the OES encodings for this number of vessels is on average lower than for four vessels. The theoretical SNR efficiency of random encoding exceeds the simulated values for random encoding in this scenario. Additional simulations (results not shown) demonstrated that OES and random encoding achieve the same SNR efficiency above the circle of Willis whether the vessels of interest were shifted or rotated.

Regardless of the number of vessels, the average SNR efficiency of the OES encodings was, on average, approximately 37% greater than for random encodings. Additionally, the minimum and maximum SNR efficiencies across all vessels for all the simulations followed the same trend as the average SNR efficiency.

Subject Scans: Four Vessels

For all subjects in both straight and rotated positions, the vascular territories were visually well

separated using both the MAP and matrix inversion analyses.

Mean SNR of the Vascular Territory Images

For images produced using the matrix inversion analysis, the OES method maintained a similar mean SNR of the vascular territory images regardless of the alignment of the subject within the magnet. According to a paired t test, the mean SNR of the OES images was significantly higher than images acquired using the random method when the subjects were aligned ($P=0.007$) and when the subjects were rotated in the standard ($P=0.013$) and random ($P=0.024$) methods (Fig. 3). The SNR efficiency of the standard method was significantly greater than random encoding in the aligned case ($P=0.010$). For images produced using the MAP analysis, similar trends were seen. Significant differences between the mean SNR of the OES and random images in the aligned ($P=0.010$) and rotated ($P=0.020$) cases were found. Similarly, the mean SNR of the standard encoding was greater than random encoding in both scenarios ($P=0.027$ in the aligned case and $P=0.008$ in the rotated case). The lack of a significant difference between the standard and OES methods is to be expected, as the MAP analysis is able to partially compensate for poorly conditioned encoding matrices (23).

Relative Labeling Efficiency Maps

The relative labeling efficiency maps revealed that the OES resulted in labeling efficiencies consistently close to the ideal values (± 1). When the subjects were rotated, the relative labeling efficiency of the standard encoding scheme images tended to move away from the ideal particularly during the anterior-posterior encodings. In this case, the vessels were both less efficiently labeled and labeled opposite to the desired encoding. Figure 4 shows a single subject example.

Subject Scans: More than Four Vessels

When labeling above the circle of Willis, it was not possible to optimally encode the vessels of interest due to

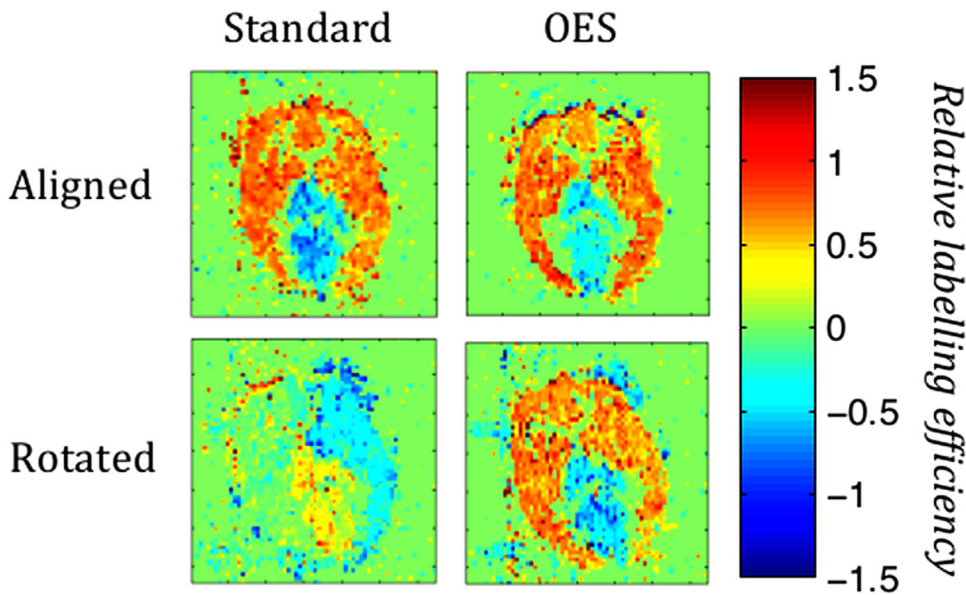


FIG. 4. Relative labeling efficiency maps for the anterior-posterior labeling of a single subject, both aligned with and rotated in the magnet.

B_0 field inhomogeneities at this level in the brain. The nonlinear inhomogeneities resulting from air in the sinuses and ear canals led to distortions in the encoding functions (Fig. 5). As a result, the vessels of interest were not labeled as expected, and only a few vascular territories were separable using MAP or matrix inversion analyses.

The labeling plane in the neck, where the two internal carotid and two vertebral arteries run approximately perpendicular to the transverse plane, does not suffer from similar levels of B_0 inhomogeneity. Multiphase PCASL (26) data from a previous study across four subjects and acquired using a labeling plane in the neck (results not shown) have found the mean absolute phase offset at this level to be approximately 0.220 ± 0.162 radians. Phase offsets of this magnitude will not interfere notably with the applied encodings.

DISCUSSION

The OES method proposed here is capable of rapidly calculating SNR optimal vessel encodings for any number and arrangement of arteries using the smallest number of possible encoding cycles. The OES has been shown in simulations and in experiments using healthy subjects to be more SNR-efficient than standard or random encoding methods when labeling four vessels, regardless of their arrangement. This is particularly useful in patient groups with irregular vascular geometry, such as subjects with arteriovenous malformations, where the vasculature can be unusual and complex. The method is computationally fast and would be simple to integrate with any scanner operating system, as it only requires basic mathematical functions and knowledge of the vessel locations.

Compared with random encoding, the OES method provides a higher SNR efficiency when labeling any

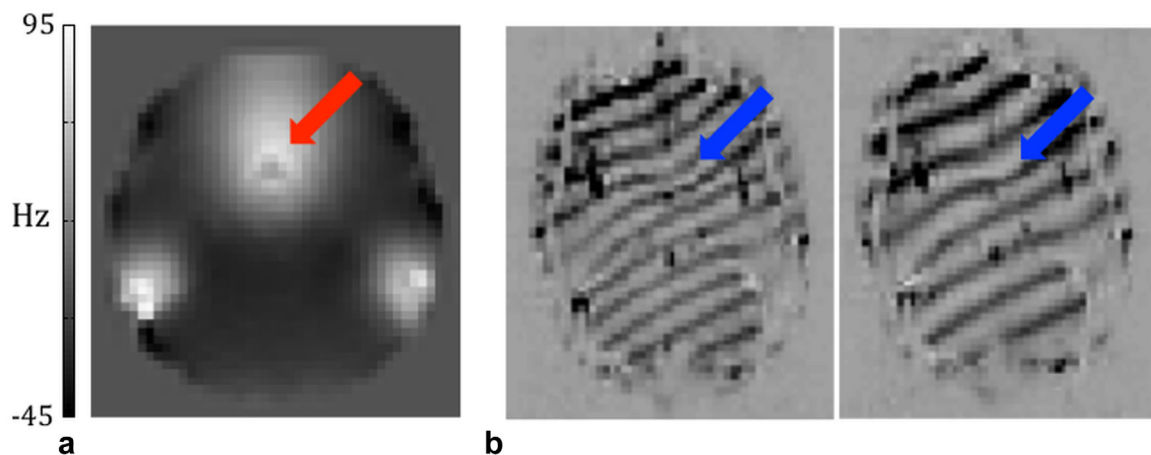


FIG. 5. **a:** Field map above the circle of Willis and **b:** two different encoding functions in a labeling plane above the circle of Willis. The largest field offsets (red arrow) cause the greatest shifts in the VEPCASL encoding functions (blue arrows).

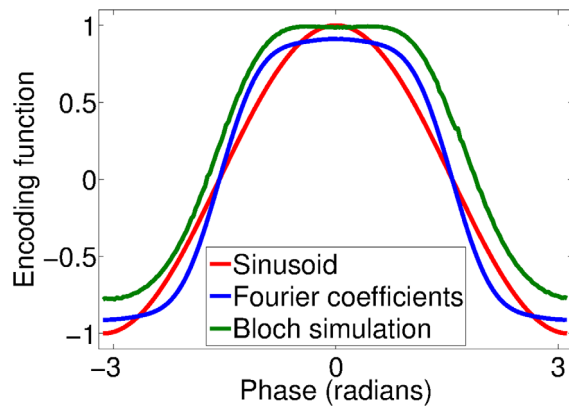


FIG. 6. The inversion efficiency of the unipolar VEPCASL pulse train, simulated using the Bloch equations for a blood velocity of $0.3 \text{ m}\cdot\text{s}^{-1}$, alongside the Fourier coefficients (scaled by 0.5) that best represent the subtraction of the labeled magnetization from the controlled magnetization for blood flow velocities between 0.05 and $0.4 \text{ m}\cdot\text{s}^{-1}$ (18) and a sinusoid.

number of vessels, while still allowing a minimal number of encodings to be used. For vessel arrangements above the circle of Willis, simulations showed that random encoding does not achieve its theoretical SNR efficiency. This may be because some of these vessels are close together and the theoretical value relates to well-separated vessels (18). Using the original random encodings (18) allowed us to compare OES with an existing method, but additional simulations (results not shown) demonstrated that including shorter wavelengths when randomly encoding nine vessels can improve the SNR efficiency. However, the mean SNR efficiency still remained significantly below that of the OES encodings. In addition, with random encoding, a high number of encodings must be performed to ensure each artery is uniquely encoded; however, it is not always possible to take the time to perform so many encodings (especially in the case of angiography, where the acquisition time is lengthy for each image). Random encoding does, however, remove the need for planning the encodings, somewhat simplifying the acquisition process. One improvement to the OES method would be to automate the input of the vessel locations into the calculation of the encodings. This would simplify and speed up the planning process. One way this could be achieved would be to use a segmentation algorithm to find the vessel locations.

It should be noted that the OES method is somewhat dependent on the choice of function used to weight the Fourier space. In the present study, a gradually varying function, with a maximum value of 0.5, was chosen so that if an encoding function with a high spatial frequency led to the most SNR-efficient encoding it was still likely to be selected, despite the weighting. However, where a number of spatial frequencies give a similar match to the desired ideal encoding, this weighting function encourages the selection of the lower spatial frequency. A linear weighting function was used in this study, but we expect that other smooth, slowly varying weighting functions would yield similar results. It is also possible to adjust the Fourier space mask according to the predicted motion of a given

subject population. This should make the OES method robust to subject motion, although if the wavelength is limited to values larger than the vessel separations, the SNR efficiency of the encodings is likely to drop.

One general limitation of this Fourier-based method is the implicit assumption that the encoding functions are sinusoids rather than a sum of Fourier coefficients. As such, it is an approximation, although both the sum of Fourier coefficients and the encoding function simulated using the Bloch equations are close to a sinusoid at the velocities typically found in the cerebral arteries (0.3 – $0.4 \text{ m}\cdot\text{s}^{-1}$ (27,28), Figure 6). It is also worth noting that the ideal encodings specify the labeling efficiency to be ± 1 at each vessel location. Therefore, as long as the peaks/troughs of the encoding function are in the correct locations, the shape of the function in between is less critical.

As with all vessel-selective methods, the OES is more likely to perform poorly if the vessels of interest are very close together. An encoding function with a sufficiently small wavelength is required to differentiate such vessels. However, if the motion of a subject is greater than the distance between vessels of interest, then vessel selectivity is not possible. The weighting and masking elements of the OES method are designed to encourage the choice of encodings that cope better with motion, while not completely excluding encodings with a wavelength small enough to differentiate vessels that are close together. If vessels are close together in a complex geometry, the use of a mask to limit the minimum possible wavelength could potentially reduce the SNR efficiency of the encodings. However, this is a reasonable tradeoff to ensure the method is more robust to subject motion. The problem of closely spaced vessels is seen to a certain extent when simulating encodings on vessels above the circle of Willis (Figure 2c), where there are a larger number of vessels close together and the average SNR efficiency does not exceed 0.75. However, this is still a considerable improvement over random encoding, where the mean SNR efficiency does not exceed 0.55.

When scanning subjects, the OES method is currently unable to provide optimal encodings for vessels above the circle of Willis due to significant B_0 field inhomogeneities at this level in the brain. However, if the true B_0 field is known, it should be possible to base an ideal encoding scheme around the desired phase at a given vessel location. In this way, the expected shifts in the encoding functions, due to field inhomogeneities, could be incorporated into the selection of the optimal spatial frequency and phase to achieve the desired encoding. This adaptation to the OES method is currently being developed.

CONCLUSIONS

We have presented a method to automatically and rapidly calculate a minimal number of optimized encodings to label any number and arrangement of vessels using VEPCASL. The OES method works well in healthy subjects when labeling four vessels in any arrangement in the neck. Adaptations will be required to allow this method to succeed in other regions, such as above the

circle of Willis, where B_0 inhomogeneities affect the position of the encoding function.

ACKNOWLEDGMENTS

We thank Dr. James Meakin for providing the multiphase PCASL data.

REFERENCES

- Liebeskind DS. Collateral circulation. *Stroke* 2003;34:2279–2284.
- van Laar PJ, van der Grond J, Hendrikse J. Brain perfusion territory imaging: methods and clinical applications of selective arterial spin-labeling MR imaging. *Radiology* 2008;246:354–364.
- Bendszus M, Koltzenburg M, Burger R, Warmuth-Metz M, Hofmann E, Solymosi L. Silent embolism in diagnostic cerebral angiography and neurointerventional procedures: a prospective study. *Lancet* 1999;354:1594–1597.
- Kaufmann TJ, Kallmes DF. Diagnostic cerebral angiography: archaic and complication-prone or here to stay for another 80 years? *AJR Am J Roentgenol* 2008;190:1435–1437.
- Okell TW, Chappell MA, Woolrich MW, Gunther M, Feinberg DA, Jezzard P. Vessel-encoded dynamic magnetic resonance angiography using arterial spin labeling. *Magn Reson Med* 2010;64:698–706.
- Davies NP, Jezzard P. Selective arterial spin labeling (SASL): perfusion territory mapping of selected feeding arteries tagged using two-dimensional radiofrequency pulses. *Magn Reson Med* 2003;49:1133–1142.
- Werner R, Norris DG, Alfke K, Mehdorn HM, Jansen O. Continuous artery-selective spin labeling (CASSL). *Magn Reson Med* 2005;53:1006–1012.
- Dai W, Robson PM, Shankaranarayanan A, Alsop DC. Modified pulsed continuous arterial spin labeling for labeling of a single artery. *Magn Reson Med* 2010;64:975–982.
- Helle M, Norris DG, Rufer S, Alfke K, Jansen O, van Osch MJ. Super-selective pseudocontinuous arterial spin labeling. *Magn Reson Med* 2010;64:777–786.
- Hendrikse J, van der Grond J, Lu H, van Zijl PCM, Golay X. Flow territory mapping of the cerebral arteries with regional perfusion MRI. *Stroke* 2004;35:882–887.
- Zimine I, Petersen ET, Golay X. Dual vessel arterial spin labeling scheme for regional perfusion imaging. *Magn Reson Med* 2006;56:1140–1144.
- Gunther M. Efficient visualization of vascular territories in the human brain by cycled arterial spin labeling MRI. *Magn Reson Med* 2006;56:671–675.
- Eastwood JD, Holder CA, Hudgins PA, Song AW. Magnetic resonance imaging with lateralized arterial spin labeling. *Magn Reson Imaging* 2002;20:583–586.
- Wong EC. Vessel-encoded arterial spin-labeling using pseudocontinuous tagging. *Magn Reson Med* 2007;58:1086–1091.
- Wu WC, Fernandez-Seara M, Detre JA, Wehrli FW, Wang J. A theoretical and experimental investigation of the tagging efficiency of pseudocontinuous arterial spin labeling. *Magn Reson Med* 2007;58:1020–1027.
- Okell TW, Chappell MA, Kelly ME, Jezzard P. Cerebral blood flow quantification using vessel-encoded arterial spin labeling. *J Cereb Blood Flow Metab* 2013;33:1716–1724.
- Wong EC, Kansagra A. Mapping middle cerebral artery branch territories with vessel encoded pseudo-continuous ASL: Sine/cosine tag modulation and data clustering in tagging efficiency space. In *Proceedings of the 16th Annual Meeting of ISMRM, Toronto, Canada, 2008*. p. 182.
- Wong EC, Guo J. Blind detection of vascular sources and territories using random vessel encoded arterial spin labeling. *MAGMA* 2012; 25:95–101.
- Gevers S, Bokkers RP, Hendrikse J, Majoie CB, Kies DA, Teeuwisse WM, Nederveen AJ, van Osch MJ. Robustness and reproducibility of flow territories defined by planning-free vessel-encoded pseudocontinuous arterial spin-labeling. *AJNR Am J Neurorad* 2012;33:E21–E25.
- Guo J, Wong EC. Optimization of the encoding scheme for improved SNR efficiency in vessel encoded pseudo-continuous ASL. In *Proceedings of the 17th Annual Meeting of ISMRM, Honolulu, Hawaii, USA, 2009*. p. 1522.
- Berry ESK, Jezzard P, Okell TW. Optimised encoding scheme for vessel-encoded pseudo-continuous arterial spin labelling. In *Proceedings of the 22nd Annual Meeting of ISMRM, Milan, Italy, 2014*. p. 721.
- Dai WY, Garcia D, de Bazelaire C, Alsop DC. Continuous flow-driven inversion for arterial spin labeling using pulsed radio frequency and gradient fields. *Magn Reson Med* 2008;60:1488–1497.
- Chappell MA, Okell TW, Payne SJ, Jezzard P, Woolrich MW. A fast analysis method for non-invasive imaging of blood flow in individual cerebral arteries using vessel-encoded arterial spin labelling angiography. *Med Image Anal* 2012;16:831–839.
- Zhang Y, Brady M, Smith S. Segmentation of brain MR images through a hidden Markov random field model and the expectation-maximization algorithm. *IEEE Trans Med Imag* 2001;20:45–57.
- Jenkinson M, Bannister P, Brady JM, Smith SM. Improved optimisation for the robust and accurate linear registration and motion correction of brain images. *NeuroImage* 2002;17:825–841.
- Jung Y, Wong EC, Liu TT. Multiphase pseudocontinuous arterial spin labeling (MP-PCASL) for robust quantification of cerebral blood flow. *Magn Reson Med* 2010;64:799–810.
- Aldo Ferrara L, Mancini M, Iannuzzi R, Marotta T, Gaeta I, Pasanisi F, Postiglione A, Guida L. Carotid diameter and blood flow velocities in cerebral circulation in hypertensive patients. *Stroke* 1995;26:418–421.
- Bammer R, Hope TA, Aksoy M, Alley MT. Time-resolved 3D quantitative flow MRI of the major intracranial vessels: initial experience and comparative evaluation at 1.5T and 3.0T in combination with parallel imaging. *Magn Reson Med* 2007;57:127–140.